In situ and time-resolved ultra small-angle neutron scattering observation on growing poly(methyl methacrylate)-*block*-polystyrene *via* reversible addition–fragmentation chain transfer living radical polymerization

Ryuhei Motokawa, Satoshi Koizumi,* Yue Zhao and Takeji Hashimoto

Soft Matter and Neutron Scattering Group, Advanced Science Research Centre, Japan Atomic Energy Agency, Japan. Correspondence e-mail: koizumi.satoshi@jaea.go.jp

Reversible addition–fragmentation chain transfer (RAFT) living radical polymerization of poly(methyl methacrylate)-*block*-polystyrene (PMMA-*b*-PS) was investigated by a combined method of gel permeation chromatography (GPC) and *in situ* and time-resolved ultra small-angle neutron scattering (tr-USANS) measurements. GPC enables us to examine a growing single molecule as a function of polymerization time, with respect to monomer conversion, molecular weight (M_n) and polydispersity index (M_w/M_n) of PMMA-*b*-PS. On the other hand, tr-USANS, observing in meso-length scales from nm to μm, reveals polymerization-induced molecular self-assembly, such as microphase separation by PMMA-*b*-PS or macrophase separation between PMMA-*b*-PS and homo-polystyrene (by-product). By combining these two experimental methods, we elucidated that RAFT living polymerization was retarded by micro- and macrophase separations.

1. Introduction

Living polymerization is a powerful method ideally suited to providing artificial polymers which are precisely controlled with respect to their monomer sequence and molecular weight (M_n), with a narrow molecular weight distribution (M_w/M_n). To achieve living polymerization, it is necessary to prohibit side reactions such as chain transfer reactions and bimolecular termination reactions. Living anionic polymerization, first discovered in the 1950s (Szwarc, 1956), is intensively utilized for precise polymer synthesis. However, there are limitations as follows: (1) living anionic polymerization is available only on non-polar hydrocarbon monomers such as styrene and 1,3-dienes, and (2) it requires perfect conditions without contaminants such as water and oxygen. Living cationic polymerization also has similar problems. To overcome these limitations for ionic polymerization, 'living radical polymerization' methods have been intensively developed during the last decade (Chiefari *et al.*, 1998; Chong *et al.*, 2003; Hawker *et al.*, 2001; Kamigaito *et al.*, 2001; Matyjaszewski & Xia, 2001) and applied to polar vinyl monomers such as methacrylates or the acrylamide group. One of the most crucial problems for radical polymerization is to prohibit bimolecular termination between radically activated growing chain ends. Reversible addition–fragmentation chain transfer (RAFT) radical polymerization (Chiefari *et al.*, 1998; Chong *et al.*, 2003) satisfies this requirement as follows: *via* weak covalent bonds, radically activated chain ends are capped by chain transfer reagents containing a dithioester functional group and stay inactive (dormant state). Thus, the concentration of active radicals decreases dramatically so that the recombination reaction is effectively prohibited.

Understanding of the reaction mechanisms of RAFT polymerization has so far been established on the assumption that the propagation reaction proceeds in a homogeneous solution, in which reacting polymers and monomers are dissolved homogeneously on a molecular level. However, in the laboratory, we often observe that viscosity or turbidity increase dramatically in the course of polymerization. These observations indirectly indicate that aggregations and/or phase-separated structures appear in the reaction solution. Especially for living radical polymerization of block copolymers, which we discuss in this paper, polymerization-induced molecular self-assembly, such as micro- and macrophase separations, occurs if the degree of polymerization N increases during the polymerization and χN exceeds a critical value for micro- and macrophase separations, where χ is the Flory interaction parameter between two different monomers (de Gennes, 1979; Hamley, 1998). Micro- and macrophase separations in the polymerization solution, which is a non-equilibrium open system, are fundamentally different from the order–disorder transition of block copolymers, induced by temperature, pressure and polymer concentration. Living polymerization might also be affected by such self-assembly.

In this paper, by employing *in situ* and time-resolved ultra small-angle neutron scattering (tr-USANS), we investigated the time evolution of micro- and macrophase separations in a reaction vessel of RAFT polymerization of poly(methyl methacrylate)-*block*-polystyrene (PMMA-*b*-PS). To realize tr-USANS, we specially built a focusing ultra small-angle neutron scattering (USANS) spectrometer with compound refractive lenses (SANS-J-II at Tokai). By time-resolved gel permeation chromatography (GPC), we investigated the time evolution of M_n and M_w/M_n of PMMA-*b*-PS. By combining

these two methods, we elucidated that the RAFT polymerization of PMMA-*b*-PS, in which PS block chains grow from the end of PMMA, was retarded when macrophase separation between PMMA-*b*-PS and homo-polystyrene (by-product) occurred.

2. Experimental methods

2.1. Materials

Methylmethacrylate (MMA) (Wako Pure Chemical Co., Osaka, Japan) was purified by distillation under vacuum. Styrene-d_8 (Aldrich) was purified with an activated alumina column to remove inhibitor. The initiator, 2,2-azobisisobutyronitrile (AIBN) (Wako Pure Chemical Co., Osaka, Japan), was purified by recrystallization from methanol. Benzene (Aldrich) was purified by distillation to use as a solvent. Cumyl dithiobenzoate (CDB; RAFT reagent) was synthesized and characterized using the procedure reported in the literature (John *et al.*, 2001; Perrier *et al.*, 2002). Using these chemical reagents, we synthesized PMMA-*b*-PS *via* RAFT living radical polymerization. As shown in the scheme below, the synthesis process is comprised of two reaction steps, *i.e.* reaction step 1 for the PMMA homopolymer and reaction step 2 for PS block chains from the PMMA end.
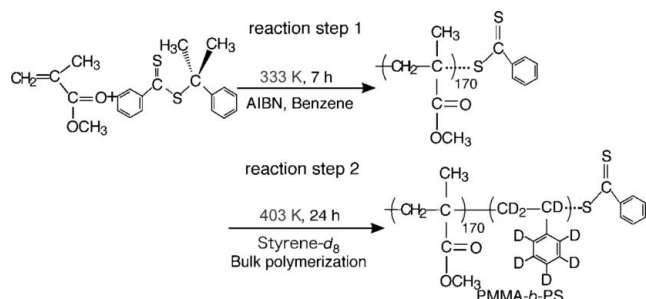
Synthesis of PMMA-*b*-PS *via* RAFT living radical polymerization

2.2. RAFT polymerization of PMMA (reaction step 1)

First, PMMA with a dithiobenzoate group at the chain end was synthesized and isolated according to the following procedures. MMA (92 mmol), CDB (0.3 mmol) and AIBN (0.1 mmol) (MMA:CDB:AIBN = 920:3:1) were dissolved in 9 ml of benzene in a 100 ml round-bottomed flask. This solution was freeze–thawed three times to remove oxygen. In an oil bath controlled at 333 K, radical polymerization was initiated without stirring. After 7 h of polymerization (MMA conversion of 34%), the solution was cooled in an ice bath and living polymerization was stopped. To remove unreacted MMA, CDB and AIBN, the polymerization solution was slowly dropped into an excess amount of methanol. The precipitate of PMMA was filtered off and then dried in a vacuum chamber. Thus, we obtained PMMA homopolymer with number-averaged molecular weight M_n = 17 000 and polydispersity index M_w/M_n = 1.1, which were determined by GPC measurements calibrated with PMMA standard. The molar ratio of PMMA with the chain end capped by a dithiobenzoate group (PMMA-RAFT) to PMMA without a cap by RAFT, PMMA-RAFT:PMMA, was evaluated as 74:26 by ^{1}H NMR measurement in chloroform-*d* at 298 K; we compared the area of proton peaks due to the methoxy group of PMMA (3.6 ppm) and to the *o*-proton of the phenyl group at the chain end (7.8 ppm).

2.3. RAFT polymerization of PMMA-*b*-PS (reaction step 2)

The isolated PMMA powder of 1.19 g, obtained after reaction step 1 and composed of a PMMA-RAFT/PMMA mixture, was dissolved in 15.7 g (0.14 mol) of styrene-d_8 in a 100 ml round-bottomed flask, which corresponds to a molar ratio of MMA:styrene-d_8 = 1:10. Note that reaction step 2 is a bulk polymerization without solvents and radical initiators. After conducting a degas operation by the freeze–thaw method, RAFT living polymerization was restarted by heating to 403 K. Radicals are generated by self-initiation of styrene monomer (Khuong *et al.*, 2005). In reaction step 2, 26% of PMMA without dithiobenzoate group caps should behave as a homopolymer.

2.4. Time-resolved GPC measurements for reaction step 2

In the course of reaction step 2, a small amount of solution was collected with a syringe under flowing dried argon gas for the GPC measurements. The collected solutions were directly diluted as 0.2 wt% tetrahydrofuran (THF) solutions without purification and injected into our GPC apparatus with a refractive index detector (TOSOH HLC-8220), operated at 313 K. Columns with three different pore sizes (Super Hz-M×2, Super Hz-2500×1 and Super Hz-1000×3; TOSOH Co. Ltd) were combined to estimate quantitatively the time-evolving M_n, M_w/M_n calibrated with PS standard, and styrene monomer conversion. THF solvent with a flow rate of 0.2 ml min^{-1} was used as the mobile phase.

2.5. Tr-USANS measurements for reaction step 2

Prior polymerization solution of 1.5 ml (PMMA-RAFT/PMMA/styrene-d_8 mixture) was poured into a quartz cell (2 mm thickness) which was connected to a three-way stopcock and vial glass tube. By heating up to 403 K in a heat block as shown in Fig. 1, tr-USANS measurements were immediately started with the SANS-J-II spectrometer installed at the JRR-3 research reactor (20 MW) at JAEA, Tokai, Japan. With a velocity selector, cold neutrons are monochromatized at wavelength λ = 0.65 nm and wavelength distribution
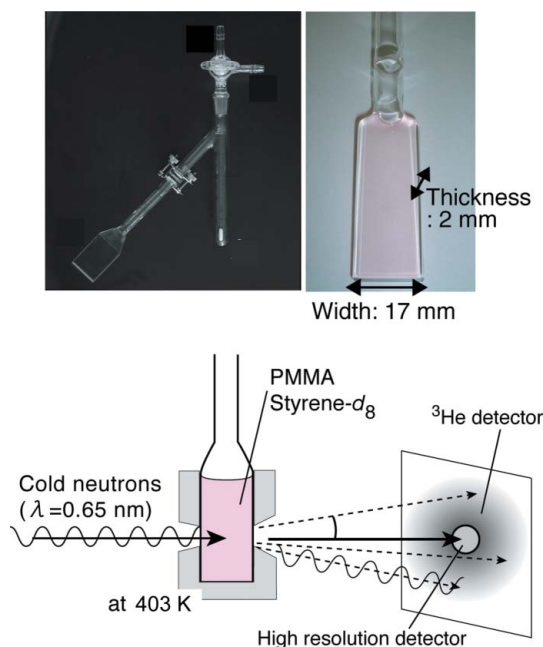

Figure 1
Experimental image and quartz cell photographs specialized for the tr-USANS observation for reaction step 2.

$\Delta\lambda/\lambda = 13\%$. On SANS-J-II, we can choose a conventional pinhole small-angle neutron scattering mode (SANS), which is able to cover the q regions of $0.03 < q < 0.25$ nm^{-1} and $0.1 < q < 1.65$ nm^{-1} by employing two detector positions (10 m and 2.5 m, respectively), where q is the modulus of the scattering vector defined by the scattering angle θ [$q = (4\pi/\lambda)\sin(\theta/2)$]. The scattered neutrons were detected by a two-dimensional position-sensitive ^{3}He detector of 0.58 m diameter and 5 mm resolution. The data were corrected for counting efficiency, instrumental background and air scattering. After circular averaging, we converted the scattering to differential scattering cross section in absolute units (cm^{-1}), using a secondary standard of irradiated Al. A focusing ultra small-angle neutron scattering mode is also available on SANS-J-II, which enabled us to access the lower q region of $0.005 < q < 0.04$ nm^{-1} by using a compound (MgF$_2$) lens and high-resolution cross-wired position-sensitive photomultiplier R3239 (5 inch size and 0.5 mm resolution, provided by Hamamatsu Photonics Co. Ltd.) with ZnS/^{6}LiF scintillator (Koizumi *et al.*, 2006).

3. Results

3.1. Time-resolved GPC measurements

As a function of monomer conversion for styrene-d_8 C_M, Fig. 2(*a*) shows M_n of PMMA-*b*-PS, determined by GPC during reaction step 2. We can clearly recognize living polymerization behavior, *i.e.* M_n increases linearly with C_M. Note that M_n with $C_M = 0$ is equal to 17 000 determined for PMMA-RAFT. Fig. 2(*b*) shows the first-order plot for reaction step 2, where the slope indicates the propagation rate constant. We recognized that the propagation rate constant changes abruptly at around polymerization time $t = 5$ h ($C_M \sim 58\%$),
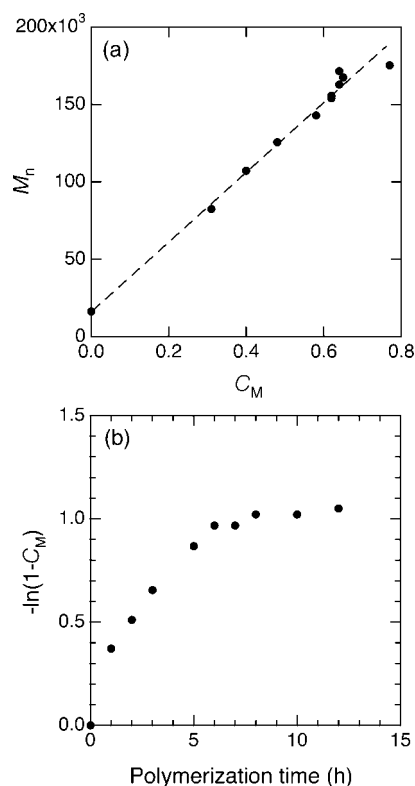
whereas the linear increase of M_n with respect to C_M does not change even after $t = 5$ h. These findings indicate that RAFT living polymerization does not change during the whole of reaction step 2. As a control experiment, we performed RAFT polymerization of polystyrene homopolymer with the same synthesis conditions as for PMMA-*b*-PS, where the change of propagation rate constant was not observed clearly. Motivated by these experimental results, obtained for a hierarchical class of single molecule, we went on to perform tr-USANS measurements focusing on reaction step 2.

3.2. Tr-USANS measurements

Fig. 3 shows the time evolution of scattering profiles obtained for reaction step 2. It is obvious that, as the polymerization time proceeds, the scattering profile changes dramatically, and we found four time regions, I to IV, as indicated in Fig. 3. At time region I at $t = 0$ h (prior to polymerization), we observed small-angle scattering due to the polymer solution of the PMMA-RAFT/PMMA mixture dissolved in styrene-d_8 monomer, where the scattering profile at low q was well reproduced by an Ornstein–Zernike type scattering function (Ornstein & Zernike, 1914). Note that styrene-d_8 behaves as a good solvent for PMMA chains. At time region II ($0 < t < 5$ h), we observed broad scattering maxima due to disordered PMMA-*b*-PS dissolved in a matrix rich in styrene-d_8 monomer. These scattering peaks originate from so-called correlation holes existing between PMMA blocks and growing PS block chains of disordered PMMA-*b*-PS (de Gennes, 1979; Leibler, 1980). As the polymerization time proceeds, the peak position q_m shifts to lower q and its intensity increases, which implies that the PS block chain grows from the PMMA end *via* RAFT living radical polymerization. At time region III ($5 < t < 7$ h), a strong upturn of small-angle scattering appears in the USANS q region ($q < 0.03$ nm^{-1}). The asymptotic decay of upturned USANS is close to q^{-4}, which is the so-called Porod law (Porod, 1951; Ruland, 1971), implying that macrophase separation occurs. It should be stressed that the focusing ultra small-angle neutron scattering mode plays a
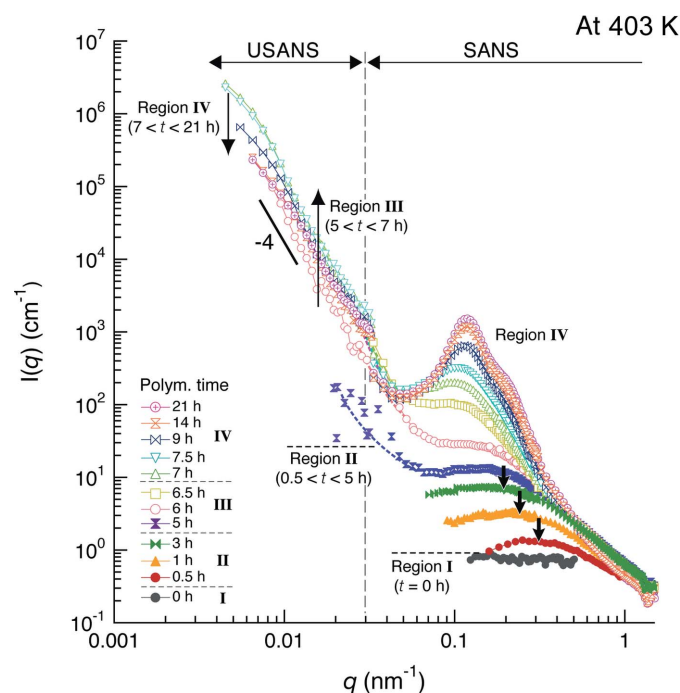

Figure 2
(*a*) M_n of PMMA-*b*-PS determined by GPC plotted as a function of styrene-d_8 monomer conversion C_M. (*b*) First-order plot for reaction step 2.

Figure 3
Ultra small-angle neutron scattering profiles obtained for *in situ* and time-resolved observations of reaction step 2.
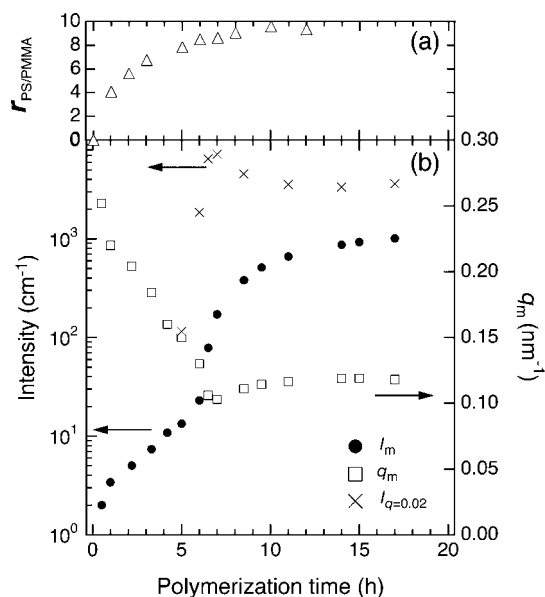
Figure 4
(*a*) Polymerization time dependence of the monomer unit ratio $r_{PS/PMMA}$ (triangles) in PMMA-*b*-PS. (*b*) The values of scattering peak intensities I_m (filled circles), position q_m (open squares) and scattering intensities at $q = 0.02$ nm^{-1} or $I_{q=0.02}$ (crosses), plotted as a function of polymerization time of reaction step 2.

crucial role in determining the asymptotic behavior of q^{-4} at $q < 0.03$ nm^{-1}. At time region III, the polymerization solution becomes turbid, which can be clearly recognized by eye. At time region IV (7 < t < 21 h), the upturned USANS decreases slightly from 7 to 10 h (see Fig. 4*b*). Simultaneously, the scattering peak intensity at q_m (at 0.1 < q < 0.5 nm^{-1}) increases abruptly with a slight shift towards higher q. This dramatic increase of peak intensity is due to microphase separation of PMMA-*b*-PS.

4. Discussion

The ratio between the degrees of polymerization for PS and PMMA block chains $r_{PS/PMMA}$ (= DP$_{PS}$/DP$_{PMMA}$, where DP is the degree of polymerization), was estimated by GPC measurements for reaction step 2 (Fig. 4*a*). After 2 h of reaction step 2, the PS block chains grow as long as the PMMA block chains. At the end of reaction step 2 ($t = 21$ h), $r_{PS/PMMA}$ becomes about 4, indicating that in the microdomains the PS block chain should behave as a corona emanating from the PMMA core.

Fig. 4(*b*) shows the time evolution of the scattering peak position q_m (squares) and its intensity I_m (filled circles), determined by tr-USANS measurements. At time region II (0 < t < 5 h), we observed a monotonic change; q_m or I_m, respectively, continue to increase or decrease linearly as a function of t. This should be attributed to disordered PMMA-*b*-PS, which is growing *via* RAFT living radical polymerization, where q_m reflects the radius of gyration averaged over all growing PMMA-*b*-PS. We found that this monotonic change in q_m and I_m continues up to 6 h, which belongs to time region III. After around 6 h, q_m becomes time-independent or shifts slightly to higher values, whereas I_m increases abruptly. According to mean field analysis using the random phase approximation, the abrupt increase of I_m at 6 h is attributed to contrast enhancement due to macrophase separation between PMMA-*b*-PS and styrene-d_8 (Motokawa *et al.*, 2007). According to GPC, C_M continues to increase after 6 h so that PMMA-*b*-PS and PS homopolymer still keep growing. The sharp

scattering peak appearing after 9 h should be attributed to microphase separation of PMMA-*b*-PS. After microphase separation in time region IV, q_m reflects the inter-domain distance between microdomains. At 7 < t < 11 h, q_m shifts toward higher q. Thus, we confirm that as the polymerization time proceeds, first macrophase separation and then microphase separation occur in the reaction solution of reaction step 2.

According to a paracrystal model analysis (Hosemann & Bagchi, 1962), we quantitatively investigated the USANS profile obtained at the end of polymerization ($t = 21$ h). The q-profile was reproduced by the paracrystal model for a spherical microdomain with body-centered cubic (BCC) symmetry (Matsuoka *et al.*, 1987; Matsuoka *et al.*, 1990). To obtain a form factor $P(q)$, we employed spherical micelles, where the PS block chains, which have a radically activated growing chain end, emanate from the PMMA core. This assumption is supported by the GPC analysis showing $r_{PS/PMMA} \simeq 4$. Thus, we obtained a radius for the PMMA core of 15.6 nm, a length of the BCC lattice of 114 nm and a g-factor = 0.12.

By the combined experimental methods of GPC and tr-USANS for the observation of reaction step 2, we found that slowing down of RAFT living radical polymerization and macrophase separation simultaneously occur at around $t = 5$ h. It might be possible that the spatial distribution of the styrene-d_8 monomer is strongly affected by macrophase and successively occurring microphase separations. In order to elucidate the macrophase separation more clearly, it is necessary to determine the solution components precisely using multi-dimensional GPC, which is our future work.

5. Summary

We performed time-resolved GPC and tr-USANS, focusing on reaction step 2 of RAFT living radical polymerization of PMMA-*b*-PS, where PS block chains are polymerized from the end of the PMMA block chains. By time-resolved GPC, we found that slowing down of RAFT polymerization occurs at $t = 5$ h. Tr-USANS, on the other hand, found that macrophase separation between PMMA-*b*-PS and PS homopolymer containing styrene monomer occurs at around $t = 5$ h. These findings suggest that living radical polymerization, occurring at atomic length scale, is strongly affected by polymerization-induced molecular self-assembly appearing in meso-length scales.

References

Chiefari, J., Chong, Y. K., Ercole, F., Krstina, J., Jeffery, J., Le, T. P. T., Mayadunne, R. T. A., Meijs, G. F., Moad, C. L., Moad, G., Rizzardo, E. & Thang, S. H. (1998). *Macromolecules*, **31**, 5559–5562.
Chong, Y. K., Krstina, J., Le, T. P. T., Moad, G., Postma, A., Rizzardo, E. & Thang, S. H. (2003). *Macromolecules*, **36**, 2256–2272.
Gennes, P. G. de (1979). *Scaling Concepts in Polymer Physics*. Ithaca, NY: Cornell University Press.
Hamley, I. W. (1998). *The Physics of Block Copolymers*. New York: Oxford University Press.
Hawker, C. J., Bosman, A. W. & Harth, E. (2001). *Chem. Rev.* **101**, 3661–3688.
Hosemann, R. & Bagchi, S. N. (1962). *Direct Analysis of Diffraction by Matter*. Amsterdam: North-Holland.
John F. Q., Ezio R. & Davis, T. P. (2001). *Chem. Commun.* pp. 1044–1045.
Kamigaito, M., Ando, T. & Sawamoto M. (2001). *Chem. Rev.* **101**, 3689–3746.
Khuong, K. S., Jones, W. H., Pryor, W. A. & Houk, K. N. (2005). *J. Am. Chem. Soc.* **127**, 1265–1277.
Koizumi, S., Iwase, H., Suzuki, J., Oku, T., Motokawa, R., Sasao, H., Tanaka, H., Yamaguchi, D., Shimizu, H. & Hashimoto, T. (2006). *Physica B*, **385–386**, 1000–1006.
Leibler, L. (1980). *Macromolecules*, **13**, 1602–1617.

Matsuoka, H., Tanaka, H., Hashimoto, T. & Ise, N. (1987). *Phys. Rev. B*, **36**, 1754–1765.

Matsuoka, H., Tanaka, H., Iizuka, N., Hashimoto, T. & Ise, N. (1990). *Phys. Rev. B*, **41**, 3854–3856.

Matyjaszewski, K. & Xia, J. (2001). *Chem. Rev.* **101**, 2921–2990.

Motokawa *et al.* (2007). In preparation.

Ornstein, L. S. & Zernike, F. (1914). *Proc. Akad. Sci. Amsterdam*, **17**, 793–806.

Perrier, S., Barner-Kowollik, C., Quinn, J. F., Vana, P. & Davis, T. P. (2002). *Macromolecules*, **35**, 8300–8306.

Porod, G. (1951). *Kolloid-Z.* **124**, 83–114.

Ruland, W. (1971). *J. Appl. Cryst.* **4**, 70–73.

Szwarc, M. (1956). *Nature*, **178**, 1168–1169.